Published on 12 August 2014. Downloaded by Library of Chinese Academy of Sciences on 08/04/2015 08:29:56.

RSC Advances

ROYAL SOCIETY OF CHEMISTRY

PAPER

View Article Online
View Journal | View Issue

Cite this: *RSC Adv.*, 2014, **4**, 39684

Hierarchical structure formation and pattern replication by capillary force lithography

H. Li,[ab] W. Yu,*[c] J. Xu,[a] C. Yang,[a] Y. Wang[a] and H. Bu[a]

Received 21st May 2014
Accepted 12th August 2014

DOI: 10.1039/c4ra04797d

www.rsc.org/advances

The soft lithographic method is gaining popularity in the manufacturing of low-cost micro and sub-microstructures. For several applications, it is desirable to fabricate structures with different lateral size as well as different height, *i.e.* hierarchical structures, on the same substrate. This is difficult for normal microfabrication methods, particularly for the photolithography method, which is the main method used in the IC industry. Here we demonstrate a simple yet cost-effective process to form hierarchical structures by capillary force lithography (CFL). In our process, the simple principle that the time needed for the fluid to fill up the cavity in the mould is different if the contact angle of the mould or the width of the cavity in the mould is different. Based on this principle, two methods were developed to achieve hierarchical structures by CFL. One is to selectively modify the PDMS mould by UV or oxygen plasma treatment to change its wettability in different areas. The other is to make patterns with variable dimensions in the mould. By using the PDMS mould with selectively modified wettability or patterns with different lateral dimensions, hierarchical structures with a convex/concave microlens array or stripes with convex/concave surfaces have been manufactured successfully.

Introduction

Photolithography has been successful in providing a way to make patterns on planar substrates in specialized polymers used as photoresists, which makes it the dominant microfabrication technology for industry in the past few decades. To overcome the limitations of photolithography and explore more cost-effective lithographic technologies, complementary non-photolithographic techniques, including nanoimprint lithography[1–3] and soft lithography[4–13] have been developed successfully during the last two decades in the field of micro- and nanofabrication.

Nanoimprint lithography employs hard moulds to impress the patterns into polymers, which has a resolution of down to a few tens of nanometers. Soft lithography is a versatile and cost-effective patterning technique used for the routine fabrication of structures with sizes down to a few tens of nanometers. Soft lithography uses elastomeric polydimethylsiloxane (PDMS) stamps to transfer a relief pattern onto the surface of a substrate by conformal contact. High-resolution soft lithography still depends on the availability of advanced lithographic techniques for stamp fabrication. CFL[14–50] is another alternative lithographic technology combining the advantages of nanoimprint and soft lithography methods.

For CFL, PDMS is used as a mould due to a number of its advantages. PDMS stamps give conformal contact over large areas, even for substrates with uneven surfaces, and are transparent, reusable and very cheap. In addition, PDMS has a very low reactivity and interfacial energy towards the polymeric materials and is sufficiently elastic so that it can be separated from the polymeric structure without destruction or distortion.

In the CFL process, as shown in Fig. 1a, a patterned (positive or negative) PDMS mould is firstly placed onto the polymer surface and then heated above the polymer's glass-transition temperature (T_g). When the polymer becomes soft, the capillarity forces of the polymer melt into the void spaces of the channels formed between the mould and the polymer, thereby generating a negative replica of the mould. When the polymer film is thick enough to completely fill the cavity of the mould, a negative replica of the mould can be obtained as shown in Fig. 2(a). However, if the polymer film is thin, relief structures with concave surfaces can be obtained as shown in Fig. 2(b).

For many applications, however, it is desirable to control the spatial arrangement of more than one component with different widths or heights in the same substrate. With traditional methods, this requires an iterative and multistep procedure, making the replication process more complex and less reliable. Here we propose a new process for fabricating hierarchical microstructures in polymeric materials by CFL. The most important concept of CFL is to take advantage of the capillary

[a]State Key Laboratory of Applied Optics, Changchun Institute of Optics, Fine Mechanics & Physics, Chinese Academy of Sciences, No.3888, Dongnanhu Road, Changchun, Jilin, P. R. China

[b]University of the Chinese Academy of Science, Beijing, 10039, P.R. China

[c]Insititue of Micro and Nano Optics, College of Optoelectronic Engineering, Shenzhen University, Shenzhen 518060, China. E-mail: yuwx_szu@163.com

This journal is © The Royal Society of Chemistry 2014

Published on 12 August 2014. Downloaded by Library of Chinese Academy of Sciences on 08/04/2015 08:29:56.

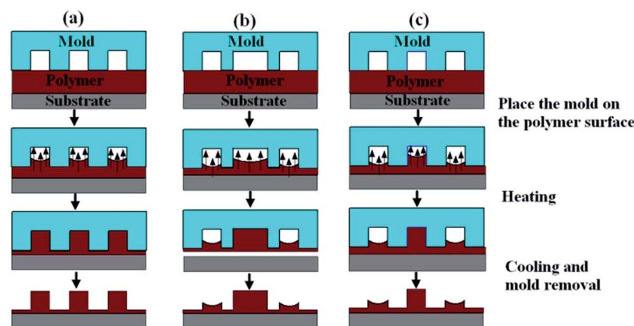

Fig. 1 Schematics of capillary force lithography: (a) pattern replication in a thick film with same size of pattern; (b) hierarchical structures fabricated using the template with patterns of different lateral dimensions; and (c) hierarchical structures fabricated using the template with different wettability distribution.

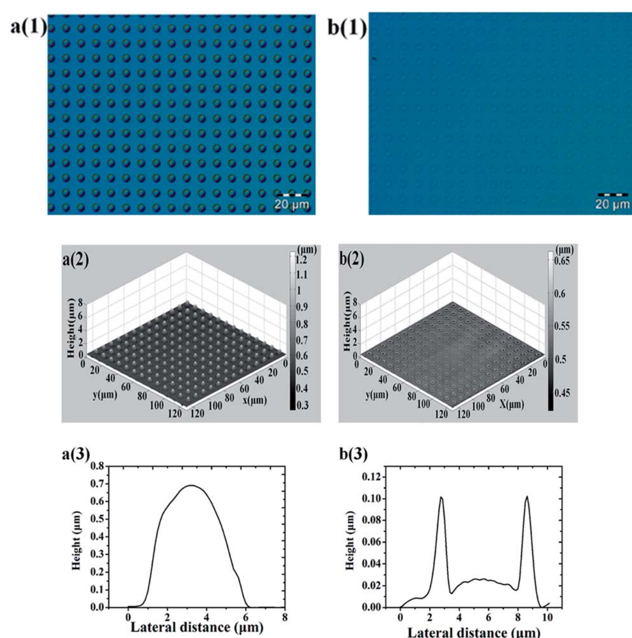

Fig. 2 Optical micrographs and 3D/2D surface profiles of the fabricated microlens (with convex surface as shown in (a), and with concave surface as shown in (b)) measured by laser scanning confocal microscope as influenced by the initial film thickness. (a) The initial S1813 film thickness is about 2.7 μm. (b) The initial S1813 film thickness is about 0.5 μm.

forces to force the polymer melt to wet the walls of the microstructures in the PDMS mould to lower the total free energy. If the interaction at the polymer/substrate interface is negligible and the polymer melt is liquid-like, the maximum height the polymer melt can rise to fill the cavity with width L by capillary action, which can be obtained by equating the capillary force to the resistant gravitational force, which gives:[51]

$$h_{\max} = \frac{2\gamma_{\text{polymer/air}} \cos\theta}{\rho G L} \tag{1}$$

where $h_{\max}$ is the maximum height, $\gamma_{\text{polymer/air}}$ is the surface tension at the polymer/air interface, θ is the contact angle at the polymer/mould interface, ρ is the density of the polymer, and G is the gravitational constant. The time it takes for the polymer melt to fill up the void spaces between the mould and the polymer film can be estimated by:[51]

$$t = \frac{2\eta z^2}{R\gamma_{\text{polymer/air}} \cos\theta} \tag{2}$$

where z is the length of the capillary to be filled, t is the time, η is the viscosity of the polymer melt, and R is the hydraulic radius (the ratio of the volume of liquid in the capillary section to the area of the solid and liquid interface), which is approximately half of the width, L. It can be seen that the amount of time needed to fill up the cavity is inversely proportional to the radius R and the cosine of the contact angle. Consequently, for the same length of the capillary z, microholes with a larger diameter and smaller contact angle will need a shorter time to fill up the cavity as shown in Fig. 1(b) and (c), respectively.

In this paper, we demonstrate a novel soft-lithographic technology using CFL for the fabrication of hierarchical structures in one step. It is found that if microholes with different diameter and the same sag height are patterned on the PDMS mould, hierarchical lateral structures that exhibit two independent characteristic dimensions can be obtained. Moreover, the surface of the PDMS mould was selected to be modified by ultraviolet radiation[52–55] or oxygen plasma treatment[56–60] so that the local wettability of the mould can be modulated to produce the hierarchical lateral structures as well. The technology demonstrated in this work might provide a simple strategy for the fabrication of hierarchical lateral structures in large-areas.

Results and discussion

Polydimethylsiloxane (PDMS, Dow Corning) was used as an elastomeric mould. A Shipley photoresist S1813 was used as the polymer to replicate the patterns in the PDMS mould. Typically, quartz glass was used as the substrate. The glass wafer was cleaned by ultrasonic treatment in acetone, alcohol and deionized water for 5 min each and dried by a stream of nitrogen. The polymer film was spin-coated onto the glass substrate and the PDMS mould was placed onto the polymers surface. In spite of the spontaneous wetting properties of the PDMS mould, care should be taken to avoid bubbles being trapped in between the mould and the polymers surface. The film was then annealed at a lower temperature. In this case, no weight or pressure was needed to keep the mould in contact with the surface.

Typically, a polymer film of S1813 was annealed at 75 °C to make the polymer chain sufficiently mobile. Since the PDMS mould has a very low reactivity with the polymer, it is quite easy to be separated from the polymeric structure. After annealing for several minutes and cooling to ambient temperature, the mould was removed from the surface and the remaining polymer structure measured a by laser scanning confocal microscope (BX61, Olympus) and optical microscope (MX61, Olympus).

Published on 12 August 2014. Downloaded by Library of Chinese Academy of Sciences on 08/04/2015 08:29:56.

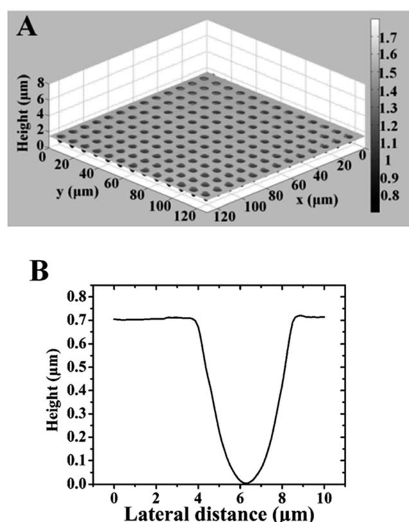

Fig. 3 3D (A) and 2D (B) surface profiles of the PDMS template fabricated with a microhole array with each microhole having a diameter of 5.75 μm and a depth of 0.7 μm. The period of the microhole array is 10 μm.

By using above process, an array of microlenses can be formed using a PDMS mould with circular holes fabricated in it. Fig. 2 shows two modes of polymer deformation as influenced by the initial polymer film thickness: a single-peak mode and a dual-peak mode. When the polymer film is thick enough, the cavity in the mould can be filled up so that a microlens with a smooth convex surface can be formed as shown in Fig. 2(a). However, if the polymer film is relatively thin (with respect to the intrusion depth of the stamp), a microlens with a smooth concave surface can be formed as shown in Fig. 2(b). In the latter case, the amount of polymer cannot fill up the cavities between the stamp and the substrate completely, as a result a meniscus shape was observed as shown in Fig. 2(b). The meniscus shape is the signature mark of the capillary rise. A microlens array with an area as large as 2 cm × 4 cm can be fabricated when the mould is in conformal contact with the polymer film. Fig. 2(a) shows the microlens array with a smooth convex surface, and each microlens has a diameter of 5.75 μm and a sag height of 0.686 μm. In this case, the initial polymer film thickness was 2.7 μm. Fig. 2(b) shows the microlens array with a smooth concave surface and each microlens has a diameter of 5.75 μm and a sag height of 76 nm. In this case, the initial polymer film thickness was only 0.5 μm. Fig. 3 shows the 3D/2D images of the PDMS template fabricated with the microhole array, which is used for the fabrication of the microlens arrays. The surface profile of the microhole was measured by a laser scanning confocal microscope and has a diameter of 5.75 μm, a sag height of 0.7 μm and a period of 10 μm.

Fig. 4 shows a serial of concave microlens arrays fabricated using the same template under different annealing temperatures. The template was patterned with square arrayed cylindrical microholes with a diameter of 45 μm and a sag height of 5 μm for each sample. As is well known, the difference in the thermal expansion coefficient between the PDMS mould and the substrate is quite large ($\alpha_{PDMS} \gg \alpha_{sub}$). High-temperature processing is known to limit the performance of PDMS stamps.[15] As a result, the mould tends to separate from the polymer surface when the annealing temperature is high. To prevent separation, the temperature was increased gradually from room temperature to the setting temperature. The thickness of the PDMS stamp was fixed at about 1.5 mm. Fig. 4 indicates how the profile of the microlens was influenced by the temperature T, ranging from 35 °C to 85 °C for the same polymer thickness (about 2.2 μm). If the polymer was annealed at 35 °C for 5 minutes, the sag height of the microlens is rather shallow. The sag height in this case was determined by the wettability of the liquid to the solid PDMS, which was characterized to have a contact angle of 6°. The sag height in this case was only 56 nm, as measured by the scanning confocal microscope. As the temperature increases, the sag height also

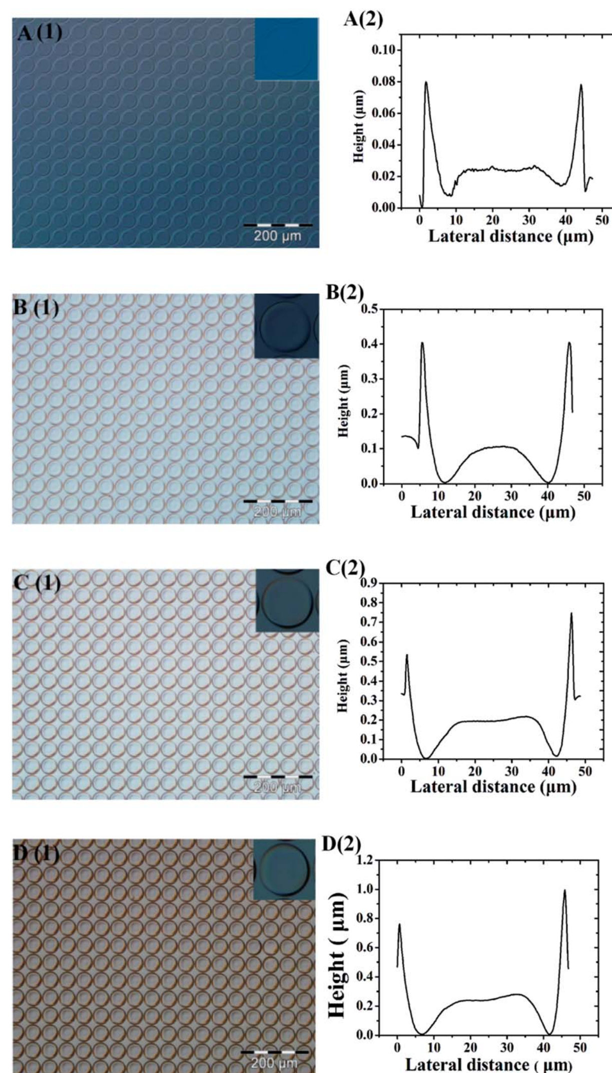

Fig. 4 The microstructures fabricated with different annealing times and at different temperatures. The pictures in the left column were taken by an optical microscope and on the right by a laser scanning confocal microscope.

 This journal is © The Royal Society of Chemistry 2014

Published on 12 August 2014. Downloaded by Library of Chinese Academy of Sciences on 08/04/2015 08:29:56.

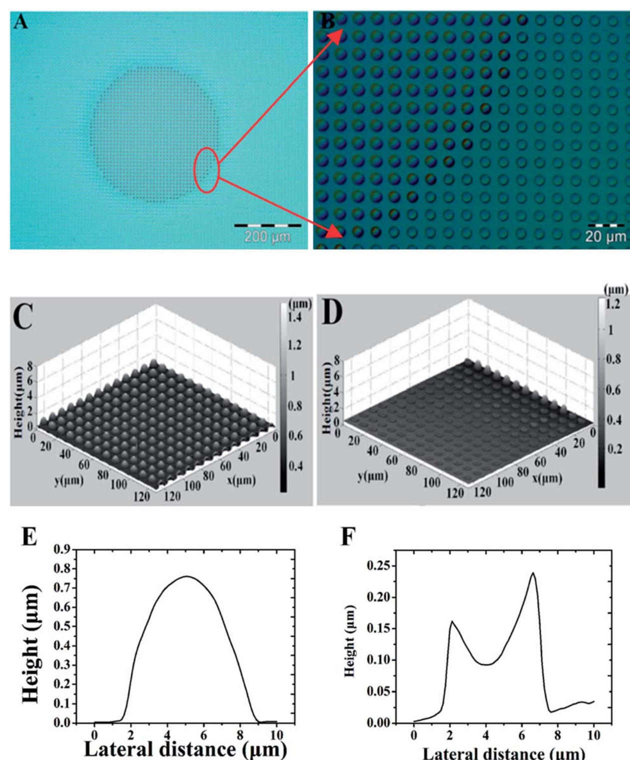

Fig. 5 Large-area images of the replicated patterns. To illustrate the fidelity of the replication process, the optical micrograph of the patterns in an area of 680 μm × 880 μm is shown in (a). The area consists of the hierarchical structure arranged on a square lattice, with convex microlens in the middle area and concave microlens in the surrounding area. Fig. 5(b) is the zoomed-in image of (a), which is used to show the hierarchical structures with different diameters. The 3D surface profiles of the fabricated microlenses were measured by a laser scanning confocal microscope and are shown in Fig. 5(c) and (d). Fig. 5(e) and (f) show the cross-sectional profiles of the microlenses with different heights at different areas.

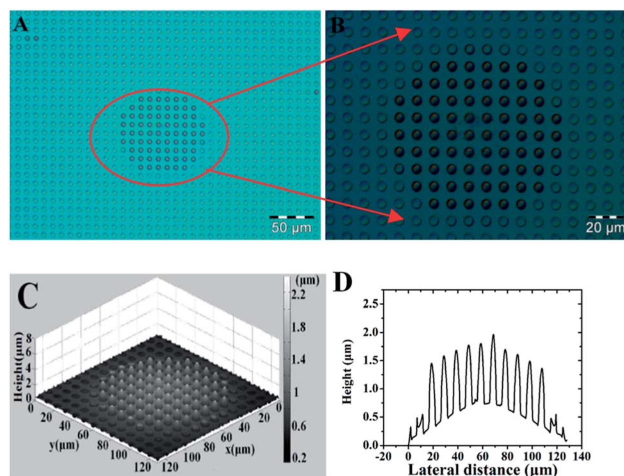

Fig. 6 Large-area images of the replicated patterns. The optical micrograph of the patterns in an area of 340 × 260 μm^2 is shown in (a). The area consists of the convex microlens arranged in a circular area and surrounded with the concave microlens. The magnified image in (b) was obtained using blue-field illumination to enhance the optical contrast. The 3D and 2D surface profiles of the fabricated microlens were measured by a laser scanning confocal microscope ((c) and (d)).

increases and was 0.3 μm for a temperature of 55 °C (Fig. 4(B)); 0.553 μm for a temperature of 75 °C (Fig. 4(C)); and 0.755 μm for a temperature of 85 °C (Fig. 4(D)).

The reliability of this structure-replication technique must be emphasized. Fig. 5(a) shows the optical micrograph of the sample with an area of 680 μm × 880 μm, which has hierarchical structures with different diameters, where the dark colour area hosts the convex microlens array with a larger diameter and the light colour area hosts the concave microlens array with a smaller diameter. Viewed at a higher magnification (Fig. 5(b)), the hierarchical structure with different diameters can be clearly seen. Fig. 5 (c)–(f) show the 3D and 2D surface profiles of the convex and concave microlens measured by a laser scanning confocal microscope (BX61, Olympus). As can be seen from Fig. 5(e), the diameter of the convex microlens is 7.625 μm, and the sag height is 0.75 μm. Fig. 5(f) shows that the concave microlens has a diameter of 6.25 μm and a sag height of 0.147 μm. The formation of the hierarchical structure of microlens at different areas was attributed to the fact that the time the polymer melt takes to fill up the void space with different size is different. Since the effect of gravity on a microscale can be ignored, the surface tension, the viscosity of the polymer melt and the size of the capillary determines the rate of flow. The flow time is given by eqn (2). It can be seen that the amount of time needed to fill the cavity is inversely proportional to the rigidity of the materials hydraulic radius R (*i.e.* the width L). Consequently, for the same length of the capillary z, a microhole with the larger diameter needs less time to fill the cavity and as a result the structure formed is higher. For the same reason, the structure formed for the microholes with a smaller diameter in the template will be lower. Therefore, the hierarchical structures with different surface profiles can be obtained.

The other way to form the hierarchical structure is to selectively modulate the wettability of the PDMS template by UV treatment. In this experiment, the microholes patterned in the PDMS template have the same diameter. Only a round area with a diameter of 120 μm in the template was illuminated by UV light for 10 min to change its wettability. The power density of UV light was about 20 mW cm^{-2}. After UV treatment, the PDMS template was placed on the polymer film with intimate contact and annealed for 6 min at 75 °C. Fig. 6(a) shows the optical micrograph of the hierarchical structures formed on the sample with an area of 680 μm × 880 μm. Fig. 6(b) shows the magnified image of the partial area in Fig. 6(a), from which one can see the distinct separation line between the different areas with different heights of microlens. Fig. 6 (c) and (d) show the 3D and 2D surface profiles of convex and concave microlens measured by a laser scanning confocal microscope (BX61, Olympus). As can be seen, the convex microlens formed in the area with UV treatment has a diameter of 6 μm and a sag height of 1.2 μm. While the area without UV treatment, the microlens has the same diameter but the sag height was only about 200 nm. Fig. 6(d) shows the convex microlens array distributed on the

Published on 12 August 2014. Downloaded by Library of Chinese Academy of Sciences on 08/04/2015 08:29:56.

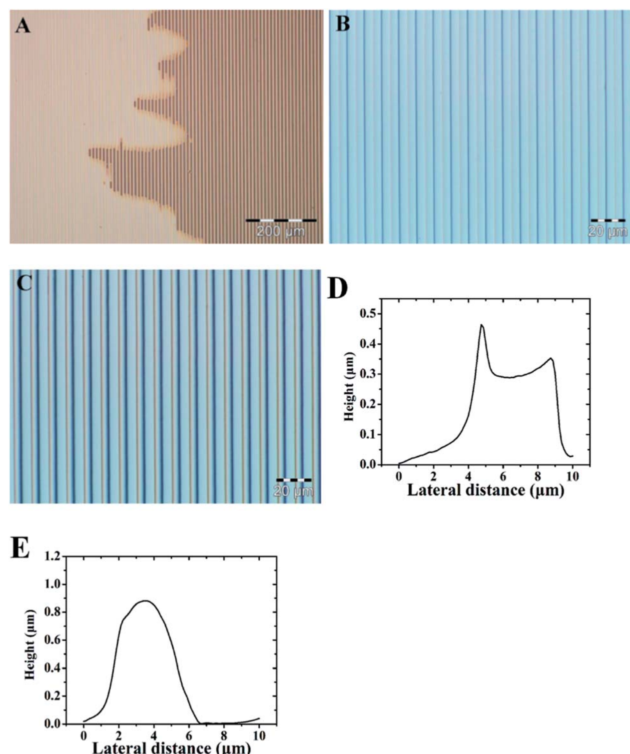

Fig. 7 The patterns formed by a partially modified PDMS mould in a 2.2 μm thick film of S1813 annealed at 75 °C for 5 min. (a) An optical micrograph of the patterns in an area of 340 × 260 μm^2. The area consists of a stripe structure with different surface profiles; (b) the magnified image of the left half of (a); (c) the magnified image of the right half of (a). (d) The 2D surface profile of the fabricated stripe in (b) measured by a laser scanning confocal microscope; (e) the 2D surface profile of the fabricated stripe in (c) measured by a laser scanning confocal microscope.

curved surface, this means that there is a difference in the hydrostatic pressure across the border between the areas with different wettability. Laplace derived an expression for the pressure difference across a curved interface in terms of the surface tension and curvature. The equation, referred to as the Laplace equation, is:[51]

$$\Delta p = p_{\text{cap}} = \frac{2\gamma \cos\theta}{r} \quad (3)$$

where Δp is the Laplace pressure, p_{cap} is the capillary driving force, γ is the surface tension, θ is the contact angle, r is the radius of the capillary. We assume that the areas with and without plasma treatment have different contact angles θ_1 and θ_2 ($\theta_1 < \theta_2$) and therefore different wettability. Because of the Laplace pressure, the pressure in the area with plasma treatment, p_1, is defined as $P_{\text{air}} - \Delta p_1$. The pressure in the area without plasma treatment, p_2, is defined as $P_{\text{air}} - \Delta p_2$. Therefore $p_2 - p_1 = \Delta p_1 - \Delta p_2 > 0$ ($\cos\theta_1 > \cos\theta_2$). This means the fluid will flow from the area with plasma treatment to that without plasma treatment. As a result, a curved surface was formed in the plasma treated area and at the same time the microlens with a convex surface was also fabricated on its surface as shown in Fig. 6(d).

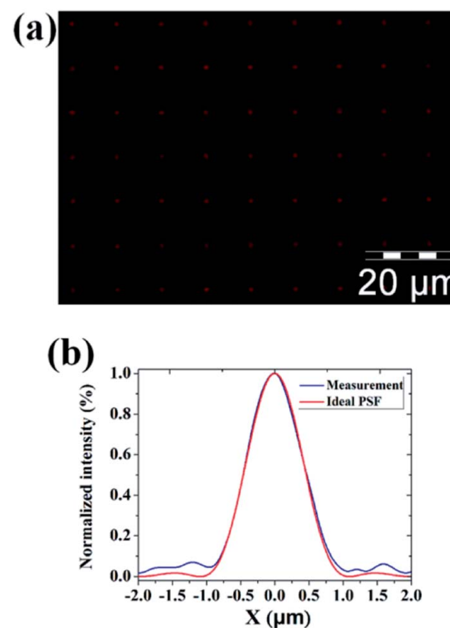

Fig. 8 The measured point spread function of the fabricated microlens shown in Fig. 2(a): (a) the measured point spread function of the fabricated microlens array, (b) comparison between the measured point spread function and the ideal diffraction-limited one.

Fig. 7 depicts the various stages of film deformation under capillary action. The partially modified PDMS mould on the wettability provides a good way to observe the evolution of film destabilization at different stages across the same PDMS mould for a fixed annealing time. The reason is that the capillary time, t, for this patterning process is inversely proportional to the cosine of the contact angle. Therefore, for a given length of cavity, the time differs if the contact angle varies, being shorter if $\cos\theta$ is larger. Oxygen plasma treatment is another method that can be used to modify the surface wettability of PDMS. Processing parameters of oxygen plasma treatment including the treatment time, radio frequency (RF) power, and oxygen flow rate influence the surface wettability of PDMS. This modification has a very short lifetime and the modified PDMS surface will recover to its hydrophobic state typically after a few hours due to the migration of short non-crosslinked PDMS chains to the surface. The typical process parameters used in oxygen plasma treatment are: a RF power of 600 W, an oxygen flow rate of 200 mL min^{-1}, and a plasma treatment time of 10 min.[60] Fig. 7(a) shows the capillary force lithography result in a 2.2 μm thick S1813 film annealed for 5 min at 75 °C. The left half of Fig. 7(a) shows the pattern obtained with the PDMS mould without plasma treatment and the right half with plasma treatment. Based on the time scale, Fig. 7(b) shows the early stage of film destabilization, forming stripes with a concave surface profile. In this case, the feature size of the strip has a width of 6.25 μm and a sag height of 0.17 μm as shown in Fig. 7(d). Fig. 7(c) shows the later stage of the film destabilization and the stripe formed has a convex surface profile. In this case, the feature size of the stripe has a width of 6.25 μm and a sag height of 0.876 μm as shown in Fig. 7(e). Apparently, the

 This journal is © The Royal Society of Chemistry 2014

Published on 12 August 2014. Downloaded by Library of Chinese Academy of Sciences on 08/04/2015 08:29:56.

different patterns shown in Fig. 7(b) and (c) were formed due to the different wettability of the PDMS mould. In the former case, the contact angle was larger and therefore the structure formed has a lower sag height and a concave surface profile. While for the latter case, the contact angle was much smaller and therefore the structure formed was much higher and has a convex surface profile. This proves that modification of the wettability of the PDMS mould by oxygen plasma treatment is an effective way to fabricate the customized patterns in different areas in the same sample.

The optical properties of the fabricated microlens array shown in Fig. 2(a) were further measured using a point spread function testing optical system. The optical system consists of a He–Ne laser, pinhole, collimating lens, 45 degree mirror and a high magnification microscope objective. Fig. 8(a) shows the image of the measured point spread function of the fabricated microlens array. The image reveals that the pitch and the intensity of the focused light spots are quite uniform. The diameter of the airy disc of the point spread function for the single microlens was found to be about 2.38 μm. Comparing with that of the diffraction limited one calculated from an ideal microlens with a diameter of 5.75 μm and a sag height of 0.686 μm, the value is very close as shown in Fig. 8(b).

Conclusions

In conclusion, we have demonstrated experimentally that capillary force lithography is a convenient and inexpensive technique for the fabrication of hierarchical structures with high fidelity and excellent uniformity without the need of advanced lithographic techniques. By applying an heterogeneous PDMS mould with different size of micro-hole arrays or selective UV or oxygen plasma treatment, hierarchical structures with different heights can be fabricated in different areas in the same sample successfully. This approach might provide a simple strategy for the fabrication of hierarchical structures with large-areas at low cost and high flexibility.

Acknowledgements

The authors acknowledge the funding from Natural Science Foundation of China under grant numbers 61361166004 and 61475156 and the Ministry of Sciences and Technology of China under grant number 2010DFR10660. Financial support from the 100 Talents Program of Chinese Academy of Sciences is also acknowledged.

Notes and references

1 S. Y. Chou, P. R. Krauss and P. J. Renstrom, *Science*, 1996, **272**, 85–87.
2 M. D. Austin, H. Ge, W. Wu, M. Li, Z. Yu, D. Wasserman, S. A. Lyon and S. Y. Chou, *Appl. Phys. Lett.*, 2004, **84**, 5299–5301.
3 S. Y. Chou, P. R. Krauss and P. J. Renstrom, *J. Vac. Sci. Technol., B: Microelectron. Nanometer Struct.*, 1996, **14**, 4129–4133.
4 A. Kumar, N. L. Abbott, E. Kim, H. A. Biebuyck and G. M. Whitesides, *Acc. Chem. Res.*, 1995, **28**, 219–226.
5 Y. Xia and G. M. Whitesides, *Angew. Chem., Int. Ed.*, 1998, **37**, 550–575.
6 E. Kim, Y. Xia and G. M. Whiteside, *Adv. Mater.*, 1996, **8**, 245–247.
7 E. Kim, Y. Xia and G. M. Whitesides, *J. Am. Chem. Soc.*, 1996, **118**, 5722–5731.
8 E. Kim, Y. Xia, X.-M. Zhao and G. M. Whitesides, *Adv. Mater.*, 1997, **9**, 651–654.
9 X.-M. Zhao, Y. Xia and G. M. Whiteside, *Adv. Mater.*, 1996, **8**, 837–840.
10 Y. Xia, P. Yang, Y. Sun, Y. Wu, B. mayers, B. Grates, Y. Yin, F. Kim and H. Yan, *Adv. Mater.*, 2003, **15**, 353–389.
11 D. Qin, Y. Xia and G. M. Whitesides, *Nat. Protoc.*, 2010, **5**, 491–502.
12 X. Gao, X. Yan, X. Yao, L. Xu, K. Zhang, J. Zhang, B. Yang and L. Jiang, *Adv. Mater.*, 2007, **19**, 2213–2217.
13 J. Aizenberg, A. J. Black and G. M. Whitesides, *Nature*, 1999, **398**, 495–497.
14 E. Kim, Y. Xia and G. M. Whitesides, *Nature*, 1995, **376**, 581–584.
15 K. Y. Suh, Y. S. Kim and H. H. Lee, *Adv. Mater.*, 2001, **13**, 1386–1389.
16 K. Y. Suh and H. H. Lee, *Adv. Funct. Mater.*, 2002, **12**, 405–413.
17 K. Y. Suh and H. H. Lee, *Adv. Mater.*, 2002, **14**, 346–351.
18 Y. S. Kim, K. Y. Suh and H. H. Lee, *Appl. Phys. Lett.*, 2001, **79**, 2285–2287.
19 S. Hun Lee, P. Kim, H. Eui Jeong and K. Y. Suh, *J. Micromech. Microeng.*, 2006, **16**, 2292–2297.
20 S.-H. Lee, H.-E. Jeong, M.-C. Park, J.-Y. Hur, H.-S. Cho, S.-H. Park and K. Y. Suh, *Adv. Mater.*, 2008, **20**, 788–792.
21 P. Kim, B. Kuk Lee, H. Yeon Lee, T. Kawai and K. Y. Suh, *Adv. Mater.*, 2008, **20**, 31–36.
22 K. Y. Suh, A. Khademhosseini, S. Jon and R. Langer, *Nano Lett.*, 2006, **6**, 1196–1201.
23 A. Khadehosseini, S. Jon, K. Y. Suh, T.-N. T. Tran, G. Eng, J. Yeh, J. Seong and R. Langer, *Adv. Mater.*, 2003, **15**, 1995–2000.
24 A. Khademhosseini, K. Y. Suh, S. Jon, G. Eng, J. Yeh, G.-J. Chen and R. Langer, *Anal. Chem.*, 2004, **76**, 3675–3681.
25 H. E. Jeong and K. Y. Suh, *J. Appl. Phys.*, 2005, **97**, 114701.
26 K. Y. Suh and R. Langer, *Appl. Phys. Lett.*, 2003, **83**, 1668–1670.
27 J. M. Karp, J. Yeh, G. Eng, J. Fukuda, J. Blumling, K.-Y. Suh, J. Cheng, A. Mahdavi, J. Borenstein, R. Langer and A. Khademhosseini, *Lab Chip*, 2007, **7**, 786–794.
28 P. Kim, D. H. Kim, B. Kim, S. K. Choi, S. H. Lee, A. Khademhosseini, R. Langer and K. Y. Suh, *Nanotechnology*, 2005, **16**, 1–7.
29 K. W. Kwon, S. S. Choi, S. H. Lee, B. Kim, Se N. Lee, M. C. Park, P. Kim, Se Y. Hwang and K. Y. Suh, *Lab Chip*, 2007, **7**, 1461–1468.
30 H. E. Jeong, R. Kwak, A. Khademhosseini and K. Y. Suh, *Nanoscale*, 2009, **1**, 331–338.

Published on 12 August 2014. Downloaded by Library of Chinese Academy of Sciences on 08/04/2015 08:29:56.

31 C. M. Bruinink, M. Peter, M. de Boer, L. Kuipers, J. Huskens and D. N. Reinhoudt, *Adv. Mater.*, 2004, **16**, 1086–1090.
32 K. Y. Suh, A. Khademhosseini, J. M. Yang, G. Eng and R. Langer, *Adv. Mater.*, 2004, **16**, 584–588.
33 A. Khademhosseini, K. Y. Suh, J. M. Yang, G. Eng, J. Yeh, S. Levenberg and R. Langer, *Biomaterials*, 2004, **25**, 3583–3592.
34 A. Khademhosseini, J. Yeh, S. Jon, G. Eng, K. Y. Suh, J. A. Burdick and R. Langer, *Lab Chip*, 2004, **4**, 425–430.
35 J.-M. Jung, F. Stellacci and H.-T. Jung, *Adv. Mater.*, 2007, **19**, 4392–4398.
36 K. Y. Suh, J. Seong, A. Khademhosseini, P. E. Laibinis and R. Langer, *Biomaterials*, 2004, **25**, 557–563.
37 D.-Y. Khang and H. H. Lee, *Adv. Mater.*, 2004, **16**, 176–179.
38 Su-K. Lee, J.-M. Jung, Ji-S. Lee and H.-T. Jung, *Langmuir*, 2010, **26**, 14359–14363.
39 K. Y. Suh, H. E. Jeong, D.-H. Kim, R. Arvind Singh and E.-S. Yoon, *J. Appl. Phys.*, 2006, **100**, 034303.
40 D.-H. Kim, P. Kim, I. Song, J. M. Cha, S. Ho Lee, B. Kim and K. Y. Suh, *Langmuir*, 2006, **22**, 5419–5426.
41 K. Y. Suh, H. E. Jeong, J. W. Park, S. H. Lee and J. K. Kim, *Korean J. Chem. Eng.*, 2006, **23**, 678–682.
42 X. Duan, Y. Zhao, A. Perl, E. Berenschot, D. N. Reinhoudt and J. Huskens, *Adv. Funct. Mater.*, 2010, **20**, 663–668.
43 H. E. Jeong, S. H. Lee, J. K. Kim and K. Y. Suh, *Langmuir*, 2006, **22**, 1640–1645.
44 D.-H. Kim, C.-H. Seo, K. Han, K. Woo Kwon, A. Levchenko and K.-Y. Suh, *Adv. Funct. Mater.*, 2009, **19**, 1579–1586.
45 H. E. Jeong, M. K. Kwak, C. I. Park and K. Y. Suh, *J. Colloid Interface Sci.*, 2009, **339**, 202–207.
46 M. C. Park, J. Y. Hur, K. W. Kwon, S.-H. Park and K. Y. Suh, *Lab Chip*, 2006, **6**, 988–994.
47 H. E. Jeong, S. H. Lee, P. Kim and K. Y. Suh, *Nano Lett.*, 2006, **6**, 1508–1513.
48 C. M. Bruinink, M. Péter, P. A. Maury, M. de Boer, L. Kuipers, J. Huskens and D. N. Reinhoudt, *Adv. Funct. Mater.*, 2006, **16**, 1555–1565.
49 C. M. Bruink, M. Peter, M. de Boer, L. Kuipers, J. Huskens and D. N. Reinhoudt, *Adv. Mater.*, 2004, **16**, 1086–1090.
50 C.-Y. Chang, S.-Y. Yang, L.-S. Huang and K.-H. Hsieh, *Opt. Express*, 2006, **14**, 6253–6258.
51 A. W. Adamson and A. P. Gast, *Physical Chemistry of Surfaces*, Wiley, New York1997.
52 K. Efimenko, W. E. Wallace and J. Genzer, *J. Colloid Interface Sci.*, 2002, **254**, 306–315.
53 C. de Menezes Atayde and I. Doi, *Phys. Status Solidi C*, 2010, **7**, 189–192.
54 B. Schnyder, T. Lippert, R. Kotz, A. Wokaun, V.-M. Graubner and O. Nuyken, *Surf. Sci.*, 2003, **532–535**, 1067–1071.
55 L. Chen, J. Ren, R. Bi and D. Chen, *Electrophoresis*, 2004, **25**, 914–921.
56 H. Hillborg, J. F. Ankner, U. W. Gedde, G. D. Smith, H. K. Yasuda and K. Wikstrom, *Polymer*, 2000, **41**, 6851–6863.
57 T. Murakami, S.-ichi Kuroda and Z. Osawa, *J. Colloid Interface Sci.*, 1998, **202**, 37–44.
58 S. Bhattacharya, A. Datta, J. M. Berg and S. Gangopadhyay, *J. Microelectromech. Syst.*, 2005, **14**, 590–597.
59 S. H. Tan, N.-T. Nguyen, Y. C. Chua and T. G. Kang, *Biomicrofluidics*, 2010, **4**, 032204.
60 Y. Xiongying, S. Liujia, Z. Rong, D. Min and F. Jinyang, *J. Tsinghua Univ.*, 2010, **50**, 1974–1977.

This journal is © The Royal Society of Chemistry 2014